Chapter 1

The Dynamical Properties on Ionic Liquids: Insights from Molecular Dynamics Study

Tateki Ishida

Additional information is available at the end of the chapter

http://dx.doi.org/10.5772/51652

1. Introduction

Ionic liquids (ILs) have attracted many researchers in the areas including physics and chemistry because of their characteristics that are different from conventional molecular liquids and, today, ILs have been one of interesting subjects of scientific study. ILs are consisted of ions and liquids at or near room temperature, and show negligible vapor pressure, thermal and chemical properties, and so on [1-8]. Also, ILs have been widely used as solvents for organic reactions with the expectation of high yields [1]. Most interesting features of ILs can be attributed to remarkable interionic interactions, and these can be an important key factor to study the characteristics of ILs at molecular level. From the results of both experimental and theoretical investigations, it has been recognized that the interionic interaction of ILs could determine physical and chemical properties.

From an experimental side, both femtosecond optically heterodyne-detected Raman-induced Kerr effect spectroscopy (OHD-RIKES)[3, 9, 10] and THz time-domain spectroscopy (THz-TDS)[11, 12] have been applied to investigate the intermolecular vibrational dynamics in ILs. In particular, with OHD-RIKES studies, the possibility to control a property such as shear viscosity by substituting an atomic element in an ionic unit has been reported [13, 14]. On the other hand, from theoretical and computational viewpoints in recent years, ILs have been chosen to study static properties such as structural and thermophysical properties[15-18] and novel interionic dynamics under solvation dynamics [19-21], dynamical properties [22-26], and Kerr spectra analyses [14, 27]. It has been suggested from the simulation studies by Ishida et al. [14] that interionic properties in ILs could be effectively adjustable by substituting an atomic unit in an ion unit in addition to a combination of cations and anions. Also, it has been pointed out that the interplay of motions between cation and anion species could play an important role in specific interionic interactions of ILs.[28]

Now, we can consider two factors important to understand specific interionic interactions in ILs. One is the interionic interaction depending on specific correlations such as cross-correlation terms between cations and anions, and the other is polarization effects due to many-body interactions caused by cations and anions in ILs. While a large number of experimental approaches have been applied to investigate these subjects, molecular-level understanding of many specific properties of ILs has been left unresolved. Obviously, theoretical researches are suitable to tackle these problems to which experimental procedures are not accessible. Thus, it is expected that such computational method as molecular dynamics (MD) simulations enables us to obtain significant information of ILs, utilizing the force field with well-parameterized potential functions and partial charges [29].

With the MD simulation procedures, it is possible to study the effects of the cross-correlations on dynamic collective motions of ions in ILs which are considered to govern the strength and behavior of couplings between ionic motions through interionic interactions [28]. The computation of the time correlations of velocity and momentum between a tagged ion and other unlike ions at different distances provides cross-correlation and momentum correlation functions [28, 30, 31]. Utilizing these calculated functions, we can investigate not only interionic interactions at molecular level but also how collective motions in ILs can proceed accompanied by the momentum transfer between ions in the target IL system.

On the other hand, electrostatic interactions between ions in ILs could be modulated due to many-body interactions and, then, it could emerge as polarization effects caused by the distortion of electron densities under anisotropic environment in ILs. It has been pointed out that the inclusion of polarization effects is significant to investigate the characteristics of ILs in structural and dynamical properties [23, 24]. Therefore, it is required for us to carry out the MD simulation, introducing such procedures as a point dipole model and a polarization energy term into the total potential energy representation of the system [32]. In addition to electrostatic interactions, describing the variation and relaxation of the polarizability anisotropy of ILs is important to investigate dynamics in ILs. For achieving this, we need to compute time-dependent polarization effects on a target system due to environmental effects in ILs. Theoretically, when we would take polarizability anisotropy into account, to track the change of molecular polarizability tensor partly dependent on molecular orientations such as rotational motions would be required. With the calculation of the time correlation function (TCF) of off-diagonal elements of the total polarizability of the system, we can investigate collective properties with the result of the polarizability anisotropy relaxation of the system.

In this chapter, we choose a 1-butyl-3-methylimidazolium cation based ILs with hexafluorophosphate anion, [BMIm][PF_6], and bis(trifluoromethylsulfonyl)amide anion, [BMIm][NTf_2], as target systems. (See Figure 1 for all the molecular structures of [BMIm]$^+$, [PF_6]$^-$ and [NTf_2]$^-$.) Firstly, we focus on the collective properties of [BMIm][PF_6] with the cross-correlation functions of ionic species in the IL and polarization effects on ionic motions. As a second, we investigate dynamical properties of [BMIm][NTf_2]. Below, we start from the explanation for the velocity cross-correlations of a central atom with neighboring atoms. Then, we show how to evaluate both cross-correlation and momentum correlation functions of the target IL. In addition, we describe the introduction of a polarization energy term and

http://dx.doi.org/10.5772/51652

the procedure to calculate induced dipole moments and the polarization energy. Following those, the theoretical background of polarization TCFs is given. Computational details are also summarized. In later sections, we discuss polarization effects on interionic interactions and specific properties related to those based on the MD simulation results. We show computation results obtained from performing MD simulation and computing the polarization TCF with the dipole-dipole (DID) approximation [4,5]. Also, we examine the relation between the anisotropic polarizability relaxation and collective motions of ionic species. Lastly, we discuss relaxation processes of ILs including an explanation of important points in studying dynamical properties on ILs.

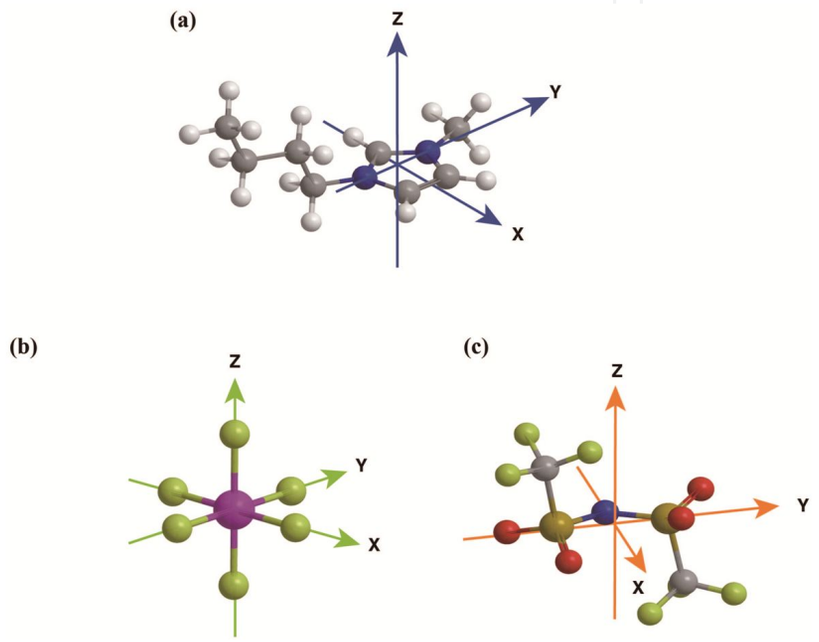

Figure 1. Molecular structures and definitions of body-fixed coordinate axes: (a) $[BMIm]^+$, (b) $[PF_6]^-$ and (c) $[NTf_2]^-$. (See text.) In $[BMIm]^+$, the *Y* direction is along the line connecting two nitrogen (blue colored) atoms in the ring, and the *Z* direction is set perpendicular to the ring plane and the *Y* direction axis. The *X* directionis set in the ring plane orthogonal to both the *Y* and the *Z* axes. In $[PF6]^-$, the *X*, *Y*, and *Z* direction axes are set equivalently. In $[NTf_2]^-$, the Y axis is along the line connecting two sulfurs (dark yellow colored), and the Z axis is set perpendicular the S-N-S plane and the X axis. The X axis is set in the S-N-S plane orthogonal to both the Y and Z axes.

2. Tracking Ionic Motions Through Interionic Interactions: Cross-Correlation, Polarization Effects, and Dynamical Properties

As mentioned in the previous section, for many problems of ILs to which experimental procedures are not accessible, theoretical investigations with computer simulation procedures are promising and suitable to obtain detailed information at molecular level. In particular, specific correlations such as cross-correlations between cations and anions seem not to be feasible to detect experimentally, but the MD simulations enable us to evaluate those. Also, for tracing dynamics in ILs such as librational and reorientational dynamics of ionic species,

cross-correlated ionic motions, and the influence of polarization coming from many-body effects caused by cations and anions in ILs from a microscopic point of view, the MD simulations are considered to be one of useful and powerful tools. In this chapter, we will show and explain the dynamical properties on ILs based on MD simulation results taking into consideration mainly following points:

1. how can cross-correlated ionic motions in ILs be modified by interionic dynamics and electronic polarizability effects ?
2. how can the collective dynamics through interionic interactions in ILs be tracked by computer simulation procedures ?
3. what kinds of properties with simulation data do we have to check and care in the investigation of dynamical properties of ILs ?
4. what kinds of subjects of ILs can be or should be investigated theoretically, considering important properties of ILs experimentally observed ?

The items 1 and 2 are main parts in this chapter, including the key results mentioned above. The item 3 is considered to be important for suggesting (or notifying) attention to researchers who are working on analyzing the dynamical properties on ILs. The item 4 includes future perspectives. In particular, we will show and discuss new aspects of ILs in each section related to the items 1, 2, and 3. Also, some of theoretical backgrounds and computational procedures for studying the dynamical properties of ILs are given in each related section, below.

At first, let us consider following points:

1. how can the collective dynamics through interionic interactions cause the unique physical and chemical properties of ILs ?
2. how can interionic dynamics be modified by electronic polarizability effects ?

The former includes the investigation of the contribution of ionic motions due to Coulombic interactions to velocity cross-correlation functions. In particular, through the analysis of the longitudinal and nonlongitudinal contributions to the velocity cross-correlation function in ILs, we will be able to investigate interionic interactions in detail. Also, important properties for physical and chemical interests such as case effects seems to be within the scope of unique collective dynamics in ILs. The later covers the relation between polarizability correlation functions and interionic interactions for ILs. To investigate these points, we can utilize useful information for static properties obtained from computer simulations, but those are not often enough to extract the details of specific interactions.

Here, we give an example that it is difficult for us to find the importance of the interactions between cation and anion species only from static properties. Figure 2 displays the computed radial distribution functions, g(r), comparing non-polarizable model with polarizable model [28]. As shown in the figure, we can observe only small difference in RDFs between two models, except that the g(r) of cation-anion is different from those of cation-cation and anion-anion as easily deduced. But, obviously, it is not feasible for us to observe information other than strong spatial correlations and sequential ordering of cation and anion pairs. In addition, the

http://dx.doi.org/10.5772/51652

analysis of averaged static structures such as RDFs is not enough to investigate remarkable polarization effects such as screening effects influenced by polarization. Below, we give a schematic explanation and discuss that to consider interionic interactions with cross-correlation analyses is important to investigate the interplay between cation and anion species in ILs, and it is shown that the cross-correlation analyses provide contrastive features.

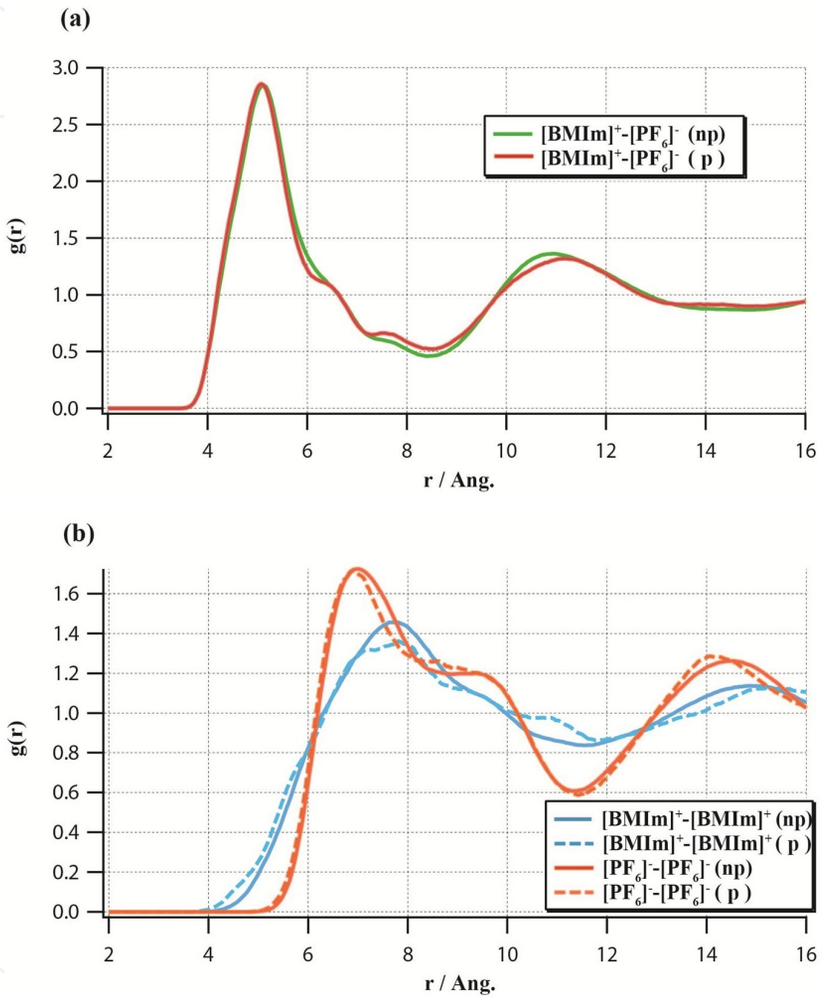

Figure 2. Radial distribution functions (rdfs) for the center of mass of [BMIm][PF_6] for both nonpolarizable (np) and polarizable (p) models: (a) $[BMIm]^+$ - $[PF_6]^-$ and (b) $[BMIm]^+$ - $[BMIm]^+$ and $[PF_6]^-$ - $[PF_6]^-$.

Different from a usual velocity autocorrelation functions (VACF), cross-correlation functions describe interactions between unlike (ionic) species (that is, between a cation and an anion in ILs) and show opposite features to VACFs. In Figure 3, these features are explained schematically. Here, it should be emphasized that cross-correlation functions provide more information on interionic interactions than that static properties such as RDFs include. As seen in Figure 3 ((a) and (b)), the variation of cross-correlation function correlates with the alteration of the VACF. In particular, the cross-correlation function shows the increasing toward the maximum peak where the VACF approaches a minimum point.

These features indicate that it is possible for us to track the time evolution of cross-correlations (between cation and anion species in ILs) as collective dynamics. In addition, it is observed in Figure 3 ((c)) that a particle (ionic species) is bouncing back and forth between like and unlike particles (ions). This implies collective (ionic) motions between coordination shells, thus, it is indicated that not only interionic interactions but also momentum transferring among ionic species could be extracted by analyzing cross-correlation functions. Also, considering that these cross-correlation functions could be modulated by the strength of interionic interactions and the coupling between cation and anion motions, cross-correlation functions would be largely influenced by polarization effects.

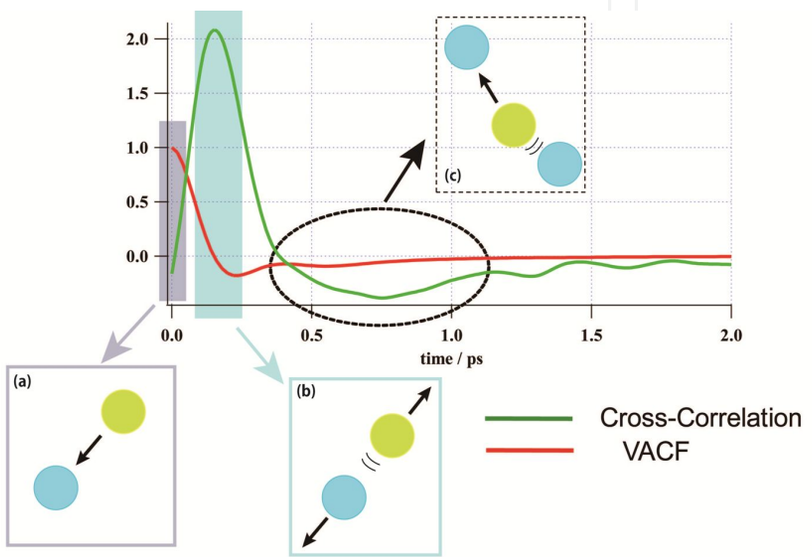

Figure 3. Schematic explanation for a cross-correlation and a VACF: (a) short-time region: an ion approaches a counter ion, and, at the same time, the VACF decreases, (b) the cross-correlation functions start decreasing after the maximum (see text) and (c) bounced ions again approaches counter ions.

On the other hand, as another type of the appearance of interplay between cross-correlation and polarization effects, we consider the polarizability anisotropy and its relaxation of an IL system. These correspond to the variation of the sum of molecular polarizability depending on time. Therefore, it is required to compute the change of molecular polarizablity on each molecule due to interionic interactions and interaction-induced multipole effects. Obviously, it is expected that molecular polarizabilites are influenced by interionic cross-correlations. In later sections, we introduce the theoretical background of polarizability TCF and its application to the study of ILs, and show how degree these are effective and discuss the importance of considering cross-correlations.

3. Theoretical Background

Here, we introduce cross-correlation functions, and then, give an explanation of a polarizable model and polarizability time correlation function. Computational details are also given.

3.1. Cross-Correlation Function

A velocity autocorrelation function (VACF) is defined for calculating the velocity correlation of a same particle as follows,

$$\mathrm{C}(t) = \langle \mathrm{v}_i(t) \cdot \mathrm{v}_i(0) \rangle \langle \mathrm{v}_i(0) \cdot \mathrm{v}_i(0) \rangle^{-1} \tag{1}$$

where $\mathrm{v}_i(t)$ is the velocity of *i*-th species. Different from the VACF, the time cross-correlation functions between the velocity of a central species *i* and the velocity of a neighboring species *j* different from the particle *i* is defined as follows [30, 31],

$$\mathrm{CR}_n^{ij}(t) = \langle \mathrm{v}_i(0) \cdot \mathrm{v}_j(t) \rangle_n \left(\langle \mathrm{v}_i{}^2 \rangle \langle \mathrm{v}_j{}^2 \rangle \right)^{-1/2} \tag{2}$$

where $\mathrm{v}_i(t)$ is the velocity of the species *i* and $\mathrm{v}_j(t)$ is the velocity of the species *j*. $\langle v_i{}^2 \rangle$and $\langle v_j{}^2 \rangle$ represent the mean square velocities. Here, it should be noted that $\langle\rangle_n$ represents a restricted statistical average [30, 31],

$$\langle \mathrm{v}_i(0) \cdot \mathrm{v}_j(t) \rangle_n = \left\langle \mathrm{v}_i(0) \sum_j \mathrm{v}_j(0) \cdot \theta\left(r_{ij}(0) - a_n\right) \cdot \theta\left(b_n - r_{ij}(0)\right) \right\rangle / N_n \tag{3}$$

where θ represents the step function. a_n and b_n are set as the positions of the *n*th minima of the radial distribution function of the system, *g(r)*. The N_n in Eqs. (2) and (3) is the coordination number in the region between $r = a_n$ and b_n. as follows,

$$N_n = 4\pi\rho \int_{a_n}^{b_n} r^2 g(r)\, dr \tag{4}$$

where ρ is the number density of the system.

Here, we can define the cross-correlation in ILs as that between a centered cation and the total contribution of other anions [28, 30],

$$\mathrm{CR}_n^{\mathrm{CA}}(t) = N_n \langle \mathrm{v_C}(0) \cdot \mathrm{v_A}(t) \rangle_n \left(\langle \mathrm{v_C}{}^2 \rangle \langle \mathrm{v_A}{}^2 \rangle \right)^{-1/2} \tag{5}$$

where "C" and "A" in super- and subscript represent cation and anion, respectively. By interchanging "C" and "A" in super- and subscript in the above equation, we can easily derive the formulation for the cross-correlation between a centered anion and other cations.

Also, with the computation of the cross-correlation functions between the velocity of a central ion and velocities of neighboring distinct ions, we can analyze the momentum transfer

between distinct ions in ILs. Introducing the momentum correlation function [28, 31], the transfer of the momentum of a cation to distinct cations and anions is defined as follows,

$$\begin{aligned} P_n^{\mathrm{C}(total)}(t) &= \left(N_n^{\mathrm{CC}} \left\langle p_+(0) \cdot p_+(t) \right\rangle_n + N_n^{\mathrm{CA}} \left\langle p_+(0) \cdot p_-(t) \right\rangle_n \right) \left(p_+^2 \right)^{-1} \\ &= P_n^{cation \to cation(\mathrm{CC})}(t) + P_n^{cation \to anion(\mathrm{CA})}(t) \end{aligned} \tag{6}$$

where p_+ and p_- mean the momentums of cation and anion, respectively. The transference of momentum of an anion to distinct anions and cations, $P_n^{\mathrm{A}(total)}$ (t), is also given as follows,

$$\begin{aligned} P_n^{\mathrm{A}(total)}(t) &= \left(N_n^{\mathrm{AA}} \left\langle p_+(0) \cdot p_+(t) \right\rangle_n + N_n^{\mathrm{AC}} \left\langle p_+(0) \cdot p_-(t) \right\rangle_n \right) \left(p_+^2 \right)^{-1} \\ &= P_n^{anion \to anion(\mathrm{AA})}(t) + P_n^{anion \to cation(\mathrm{AC})}(t) \end{aligned} \tag{7}$$

3.2. Polarization Effects

3.2.1. A Polarizable Model

Here, we introduce a polarizable model considering induced dipole moments and explain the procedure for computing induced dipole moments and the many-body polarization energy [33-35].

The total potential energy of the system under the resulting polarizable force field is defined as follows,

$$V_{tot} = V_{bond} + V_{nonbond} + V_{pol} \tag{8}$$

where the terms V_{bond} and $V_{nonbond}$ are intra- and intermolecular interaction energies. The polarization energy, V_{pol}, is decomposed into the three terms as follows,

$$V_{pol} = V_{charge-dipole} + V_{dipole-dipole} + V_{self} \tag{9}$$

where the charge-dipole contribution, $V_{charge\text{-}dipole}$, the dipole-dipole contribution, $V_{dipole\text{-}dipole}$, and the self-polarizability term, V_{self}, are defined, respectively, as

$$V_{charge-dipole} = -\sum_i \mu_i \cdot E_i \tag{10}$$

$$V_{dipole-dipole} = \sum_{i>j} \mu_i \cdot T_{ij} \cdot \mu_j \tag{11}$$

http://dx.doi.org/10.5772/51652

$$V_{self} = \sum_i \frac{1}{2\alpha_i} \mu_i \cdot \mu_i \tag{12}$$

In the above equations, E_i is the electric field on atom *i*, produced by the partial charges of all other surrounding atoms, and μ_i represents the induced dipole moment on atom *i*. Also, $\alpha_i$means the isotropic atomic polarizability of atom *i*. In Eq. (11), the T_{ij}, is the dipole field tensor element defined as follows,

$$T_{ij} = \frac{1}{r_{ij}^3}\left[1 - \frac{3\mathbf{r}_{ij}\mathbf{r}_{ij}}{r_{ij}^2}\right] \tag{13}$$

where $r_{ij} = r_i - r_j$. The induced dipole moment on atom *i* is given by

$$\mu_i = \alpha_i\left(E_i - \sum_{j\neq i} T_{ij}\mu_j\right) \tag{14}$$

With Eqs. (10), (11), and (12), the polarization energy, E_{pol}, is summarized as follows,

$$V_{pol} = -\frac{1}{2}\sum_i \mu_i \cdot E_i \tag{15}$$

3.2.2. Polarizability Time-Correlation Function (TCF)

The polarizability anisotropy of the system can be tractable by calculating the TCF of off-diagonal elements of the total polarizability. Here, the theoretical background of the polarizability TCF is summarized briefly.

At first, we define the total polarizability of the system, $\Pi(t)$, that is the sum of the molecular polarizability, $\Pi^M(t)$, and the interaction-induced polarizability, $\Pi^{II}(t)$, as follows,

$$\Pi(t) = \Pi^{M}(t) + \Pi^{II}(t) \tag{16}$$

where *t* represents the time dependence, and subscripts M and II mean the molecular part and the interaction-induced part, respectively. The molecular part is given by the sum of the polarizability tensors of isolated gas phase molecular polarizability in the laboratory frame,

$$\Pi^{\mathrm{M}}(t) = \sum_{i=1}^{N} \alpha_i(t) \tag{17}$$

where N is the number of molecules, and α_i is the polarizability tensor of molecule i. For the formulation of the interaction-induced part, we employ the dipole-induced-dipole (DID) model approximation [36, 37], which assumes that the molecular polarizabilities are modified due to a dipolar coupling with the influence of higher order unconsidered. The interaction-induced polarizability in the DID approximation is given as follows,

$$\Pi^{\mathrm{II}}(t) = \sum_{i=1}^{N} \sum_{j \neq i}^{N} \alpha_i(t) \cdot T_{ij}(t) \cdot \tilde{\alpha}_j(t) \tag{18}$$

where T_{ij} means the dipole interaction tensor between molecules i and j. $\tilde{\alpha}_i(t)$is the effective polarizability for molecule i defined by the following equation including the interaction-induced effects,

$$\tilde{\alpha}_i(t) = \alpha_i(t) + \sum_{j \neq i}^{N} \alpha_i(t) \cdot T_{ij}(t) \cdot \tilde{\alpha}_j(t) \tag{19}$$

Equation (19) can be solved by the calculation procedure that is called the all-orders DID approximation [37]. It should be noted that the DID model employed here assumes a center-center DID model, where it recognizes the polarizability as concentrated in the center of mass of the molecule.

Here, we give the representation of the total system polarizability including the cationic and anionic components [14, 27],

$$\Pi(t) = \Pi^{\mathrm{C}}(t) + \Pi^{\mathrm{A}}(t) \tag{20}$$

where the superscripts C and A represent cation and anion species, respectively. Referring to Equations. (16), (17), and (18), the $\Pi^{C}(t)$ and $\Pi^{A}(t)$ defined as follows,

$$\Pi^{\mathrm{C}}(t) = \sum_{i=1} (\alpha_i^{\mathrm{C(M)}}(t) + \alpha_i^{\mathrm{C(II)}}(t)) \tag{21}$$

$$\Pi^{\mathrm{A}}(t) = \sum_{j=1} (\alpha_j^{\mathrm{A(M)}}(t) + \alpha_j^{\mathrm{A(II)}}(t)) \tag{22}$$

where the indices *k* and *l* go over all cations and anions, respectively. Then, the total polarizability of the system, $\Pi(t)$, can be rewritten, as follows,

$$\begin{aligned}\Pi(t) &= \frac{1}{3}\mathrm{Tr}\left(\Pi^{\mathrm{C}}(t)+\Pi^{\mathrm{A}}(t)\right)\mathbf{I} \\ &+\left\{\Pi^{\mathrm{C}}(t)-\frac{1}{3}\mathrm{Tr}\left(\Pi^{\mathrm{C}}(t)\right)\mathbf{I}\right\}+\left\{\Pi^{\mathrm{A}}(t)-\frac{1}{3}\mathrm{Tr}\left(\Pi^{\mathrm{A}}(t)\right)\mathbf{I}\right\} \\ &= \frac{1}{3}\mathrm{Tr}\left(\Pi^{\mathrm{C}}(t)+\Pi^{\mathrm{A}}(t)\right)\mathbf{I}+\beta^{\mathrm{C}}(t)+\beta^{\mathrm{A}}(t)\end{aligned} \tag{23}$$

Where $\beta^{\mathrm{C}}(t)=\left\{\Pi^{\mathrm{C}}(t)-\frac{1}{3}\mathrm{Tr}\left(\Pi^{\mathrm{C}}(t)\right)\boldsymbol{I}\right\}$ and $\beta^{\mathrm{A}}(t)=\left\{\Pi^{\mathrm{A}}(t)-\frac{1}{3}\mathrm{Tr}\left(\Pi^{\mathrm{A}}(t)\right)\boldsymbol{I}\right\}$ and $\boldsymbol{I}$ is the unit tensor. Finally, the polarizability TCF, $\phi(t)$, can be rewritten as follows,

$$\begin{aligned}\phi(t) &= \left\langle \mathrm{Tr}\left[\left(\beta^{\mathrm{C}}(0)+\beta^{\mathrm{A}}(0)\right)\cdot\left(\beta^{\mathrm{C}}(t)+\beta^{\mathrm{A}}(t)\right)\right]\right\rangle \\ &= \left\langle \mathrm{Tr}\left(\beta^{\mathrm{C}}(0)\cdot\beta^{\mathrm{C}}(t)\right)\right\rangle+\left\langle \mathrm{Tr}\left(\beta^{\mathrm{A}}(0)\cdot\beta^{\mathrm{A}}(t)\right)\right\rangle \\ &+\left\langle \mathrm{Tr}\left(\beta^{\mathrm{C}}(0)\cdot\beta^{\mathrm{A}}(t)\right)\right\rangle+\left\langle \mathrm{Tr}\left(\beta^{\mathrm{A}}(0)\cdot\beta^{\mathrm{C}}(t)\right)\right\rangle \\ &= \phi^{\mathrm{C}}(t)+\phi^{\mathrm{A}}(t)+\phi^{\mathrm{C\text{-}A}}(t)\end{aligned} \tag{24}$$

where

$$\begin{aligned}\phi^{C}(t) &= \langle \mathrm{Tr}(\beta^{C}(0)\cdot\beta^{C}(t))\rangle \\ \phi^{A}(t) &= \langle \mathrm{Tr}(\beta^{A}(0)\cdot\beta^{A}(t))\rangle \\ \phi^{C-A}(t) &= \langle \mathrm{Tr}(\beta^{C}(0)\cdot\beta^{A}(t))\rangle+\langle \mathrm{Tr}(\beta^{A}(0)\cdot\beta^{C}(t))\rangle\end{aligned}$$

The nuclear response function, $R(t)$, is represented as the time derivative of the polarizability TCF,

$$R(t) = -\frac{1}{k_B T}\frac{\partial}{\partial t}\phi(t) \tag{25}$$

3.3. Computational Details

Utilizing the sets of force field parameters for $[BMIm]^+$, $[PF_6]^-$ and $[NTf_2]^-$ [38-40], MD simulations have been performed with the DL_POLY molecular dynamics suite [41]. In all the simulations, all the stretching bonds were constrained with the SHAKE algorithm [42]. 125 ion pairs (4000 atoms for $[BMIm][PF_6]$ and 5000 for $[BMIm][NTf_2]$) were set in a cubic box under the periodic boundary condition. The lengths of cubic box size were set to be 35.47

and 38.46 Å to reproduce the experimental data of the densities of [BMIm][PF_6] and [BMIm][NTf_2] at 298 K [13, 43]. 12 Å was set as cutoff length. The time step was 2 fs. The long-range Coulomb and polarization terms were computed with the Ewald's summation technique [44]. Firstly, each system was equilibrated at 600 K for 15 ns in the NVE run and then successively cooled down to 298 K in several stages using velocity scaling. Then, 20 ns NVT run for equilibration at 298 K was carried out. After these equilibration runs, trajectories were recorded every 20 fs (50 fs for [BMIm][NTf_2]) and collected during 10 ns (20 ns for [BMIm][NTf_2]) production runs. For atomic polarizabilities, from the literature [45, 46], we adopted 1.152, 0.705 and 0.0885 Å^3 for the C, N, and H atoms of the cation, respectively, and 0.121 and 3.630 Å^3 for the F and P atoms of the anion, respectively. We considered the distance and vector between the atomic sites of distinct molecules in the dipole interaction tensor, $\mathrm{T}=(\boldsymbol{I}-3\hat{\boldsymbol{r}}\hat{\boldsymbol{r}})/r^3$, where $\hat{\boldsymbol{r}}=\boldsymbol{r}/r$ Then, the range of the attenuation of dipolar interactions at short distances, s, was evaluated with the Thole's definition [47], $s = 1.662(\alpha_i\alpha_j)^{1/6}$ with atomic polarizabilities, α_i and α_j. Also, the dipole interaction tensor we used is given by [47]

$$\mathrm{T} = (\mathbf{I} - 3\hat{\mathbf{r}}\hat{\mathbf{r}})/r^3 \quad (r > s) \tag{28}$$

$$\mathrm{T} = \left[(4\mathrm{a}^3 - 3\mathrm{a}^4)\mathbf{I} - 3\mathrm{a}^4\hat{\mathbf{r}}\hat{\mathbf{r}}\right]/r^3 \quad (r \le s) \tag{29}$$

where a = r/s. Equation (14) is solved with an iterative procedure at each time step, and then, the criterion value of iterative solution for induced dipole moment was set to 0.001 D. For the computation of the polarizability TCF of [BMIm][NTf_2], we used molecular polarizabilities of 14.372 Å^3 for [BMIm]$^+$ and 11.259 Å^3 for [NTf_2]$^-$.[48] The body-fixed coordinate axes set in the cation and the anion are shown in Figure 2. For more computational procedures in detail, interested readers should refer to references [14] and [28].

4. Cross-Correlation, Momentum Correlation, and Polarization Effects

The computed velocity cross-correlation functions [28] are shown in Figures 4 and 5. These figures show the comparison of velocity cross-correlation functions observed around the cation, [BMIm]$^+$, and the anion, [PF_6]$^-$, placed at the center, for both the nonpolarizable and polarizable models. From the result of the cation-anion RDF in Figure 2, we selected 3.5, 8.4, 8.4, and 14.75 Å for the value of a_1, b_1, a_2, and b_2 in Equation (4) for the nonpolarizable model, respectively, and 3.5, 8.5, 8.5, and 15.0 Å for the polarizable model, respectively. With these values, the first (C_1(t)) and second (C_2(t)) coordination shells were specified. It should be noted that the C_1(t) between the center anion and distinct anions is not shown in Figure 5 because the C_1(t) is almost zero corresponding to the result that the anion-anion RDF result is almost zero at the region of the specified first coordination shell (see RDFs in Figure 2(b)). Also, it should be noted that the initial values, $C_n(0)$, are negative since the system size is finite as have been pointed out [30].

http://dx.doi.org/10.5772/51652

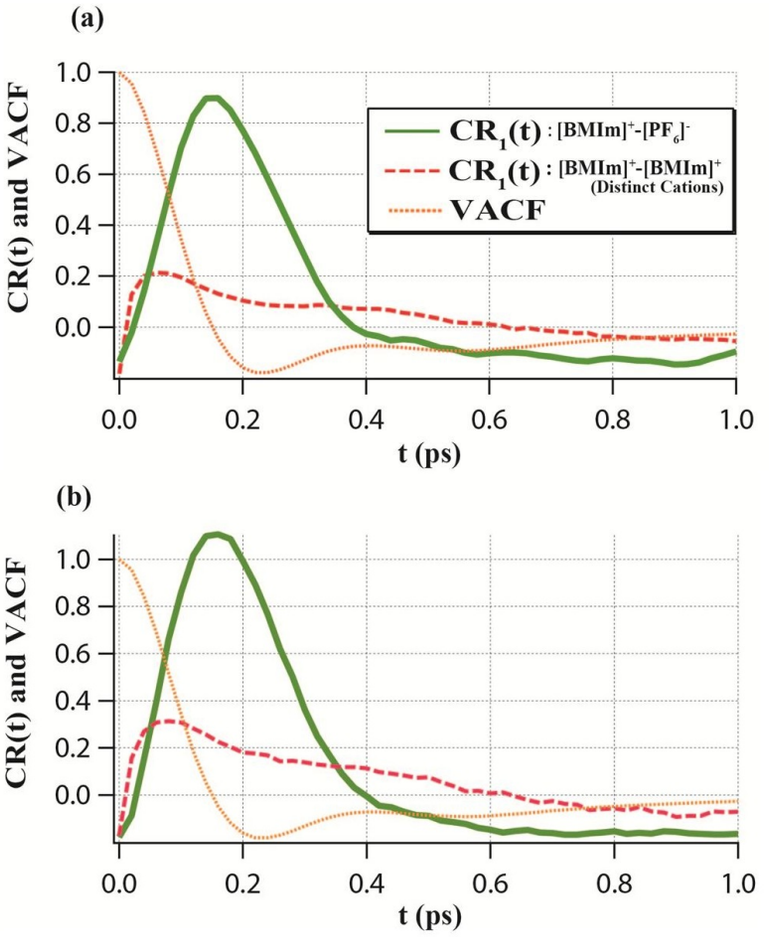

Figure 4. The Calculated velocity cross-correlation functions between the $[BMIm]^+$ set at the center in the first coordination shell and $[PF_6]^-$, and between the center cation and other cations, including VACF: (a) in the nonpolarizable model and (b) in the polarizable model.

As shown in Figures 4 and 5, the VACFs are also displayed for comparison. As briefly explained in Section 2 with Figure 3, the initial rise of the cross-correlation function, $C_1(t)$, appears toward the maximum for both models, corresponding to the decay of the VACF to the minimum (see the (a) and (b) in Figure 3). These results indicate that the initial momentum of the central ion is gained by neighboring ions immediately after t = 0. In addition, following decay profiles (see the (c) in Figure 3) are seen. These are ascribed to the spread of transferred momentum to the outer coordination shells. The peak height of the $C_1(t)$ in the polarizable model is larger than that in the nonpolarizable model. These significant results indicate that the momentum transfer can be intensified from the more distant coordination shells to the first ones due to both the charge-dipole and dipole-dipole interactions by polarization effects in addition to charge-charge Coulomb interactions. As the characteristics of the VACF profile, it is noted that the minima of the VACF are located at the positions later than those of the maxima of the velocity cross-correlation functions for the first coordination shell. These features imply that the momentum transmitted to the neighbors at the first shell is regained partly by the central cation or anion, bounc-

ing back and forth for some time, as have been pointed out in the literature on the computer simulations of simple liquid binary mixtures [28, 31].

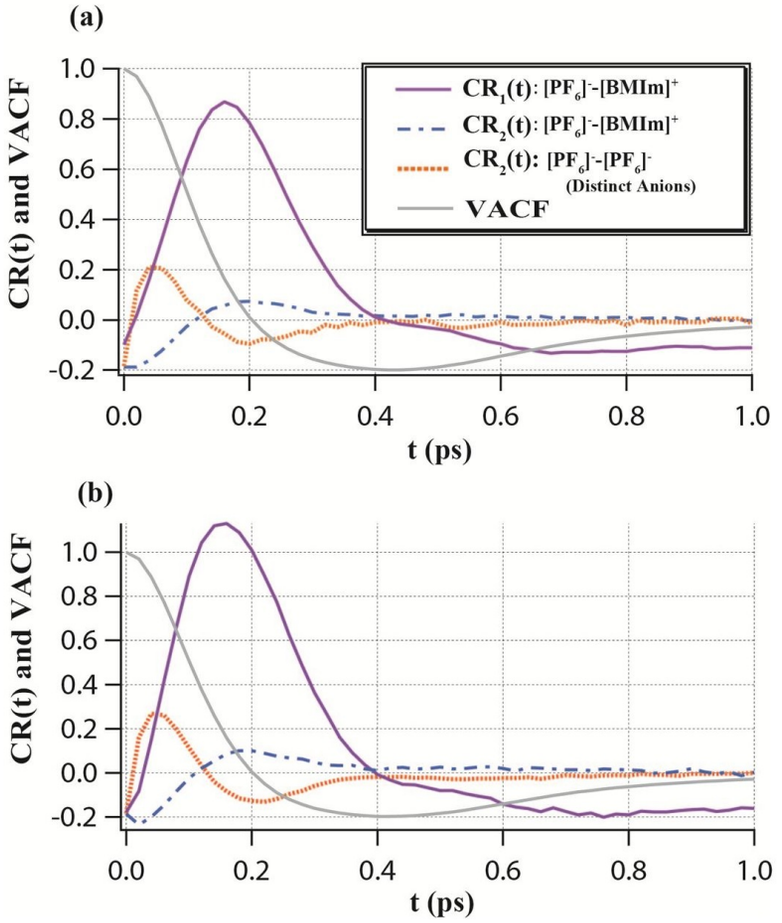

Figure 5. The Calculated velocity cross-correlation functions between the $[PF_6]^-$ set at the center in the first and second coordination shells and $[BMIm]^+$, and between the center anion and anions, including VACF: (a) in the nonpolarizable model and (b) in the polarizable model.

On the other hand, an interesting feature is seen in the $C_1(t)$ between distinct cations (or the $C_2(t)$ for distinct anions). As indicated in Figures 4 and 5, the cross-correlation function for distinct ions reaches the maximum point earlier than the $C_1(t)$ for the cation-anion cross-correlation, even though the peak height is smaller than that in the cation-anion cross-correlation function. On these results, it is considered that the alteration of cage effects increases the probability that a cation (or an anion) meets a distinct cation (or anion) at early time region.

Also, in Figures 4 and 5, it is clearly observed that the cross-correlation function between distinct like ions is influenced by the modulation of cage effects due to polarization effects and that its peak height is enhanced in the polarizable model [28]. As shown in Figures 4 and 5, when VACFs pass the value of zero to negative, the cross-correlation functions reach the maximum point. Thus, this implies that the central cation (or anion) is likely to lose its initial momentum. In addition, as seen in Figure 5, the peak position of $C_2(t)$ is shifted to the

http://dx.doi.org/10.5772/51652

time region later than that of $C_1(t)$. This is consistent with the consideration that the momentum of the central ion is transferred from the first coordination shell to the second.

Here, we examine the characteristics of the cross-correlation functions. As shown in Figure 6, we consider the decomposition of a cross-correlation function into the longitudinal (denoted as L in the figure), $C_n^{L}(t)$, and nonlogitudinal (denoted as NL in the figure), $C_n^{NL}(t)$, contributions as follows [28, 31, 49],

$$CR_n(t) = CR_n^{L}(t) + CR_n^{NL}(t) \tag{30}$$

where $CR_n^{L}(t)$ is represented as the velocity cross-correlation along the direction designated by the center of masses of distinct ions at t = 0. We can compute $CR_n^{L}(t)$ with the following equation [28, 31, 49],

$$CR_n^{L}(t) = N_n \left\langle v_i^{L}(0) \cdot v_j^{L}(t) \right\rangle_n \left(\left\langle v_i^{2} \right\rangle \left\langle v_j^{2} \right\rangle \right)^{-1/2} \tag{31}$$

where $v_i^{L}(t) = v_i(t)[r_{ij}(0)/r_{ij}(0)]$ and $v_i(t)$ is the velocity of the ionic species *i*. Also, $r_{ij}(0)$ means the direction vector between the center of masses of the distinct ions i and j. $\langle v_i^2 \rangle$and $\langle v_j^2 \rangle$ represent the mean square velocities. $CR_n^{NL}(t)$ can be computed with $CR_n(t)$ and $CR_n^{L}(t)$. Figure 7 shows the computed $C_n^{L}(t)$ and $C_n^{NL}(t)$ functions for a centered cation at the first coordination shell (n = 1) both for the nonpolarizable and polarizable models [28]. All the results indicate that the velocity cross-correlations at the short time region up to 0.4 ps are predominantly governed by the longitudinal function, $C_n^{L}(t)$.

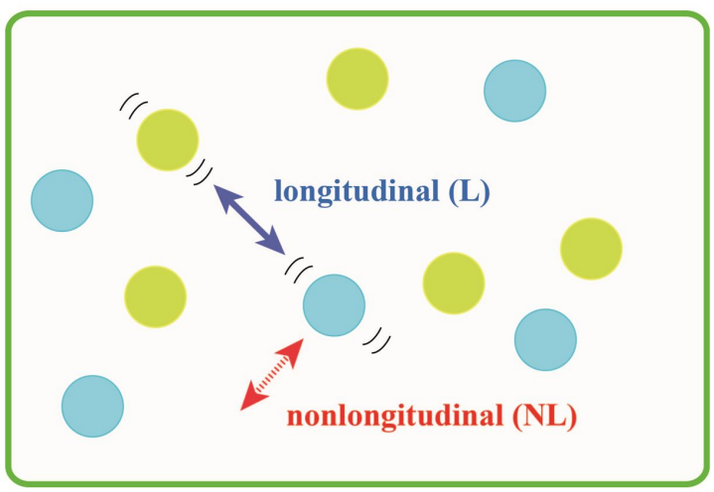

Figure 6. Schematic explanation of the longitudinal (L) and nonlongitudinal (NL) of a cross-correlation function.

These results clearly indicate that the Coulomb interactions between neighboring ions are mainly effective on the ionic motions as "driving forces" at the short time. In addition, the

magnitude of the longitudinal correlation of ions in the polarizable model is larger than that in the nonpolarizable model. Therefore, it is considered that the longitudinal motions are strongly affected by polarization effects. On the decay behavior, similar features are obtained in both models. These indicate that polarization effects on the longitudinal motion complete mostly at the short time region.

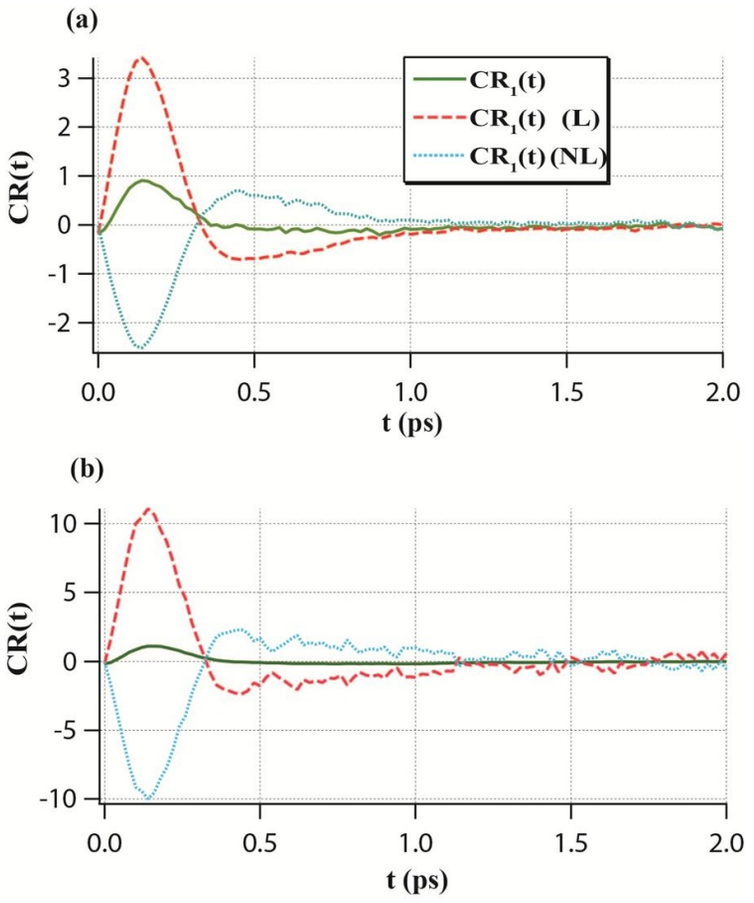

Figure 7. The simulated longitudinal and nonlongitudinal contributions to the velocity cross-correlation function: (a) in the nonpolarizable model and (b) in the polarizable model.

Next, the computed results of momentum correlation functions [28] are displayed in Figures 8 and 9. As shown in Figures 8 and 9 in common, the initial momentum of the cation (or anion) is mainly transferred to the close anions (or cations) while the momentum correlation with distinct cations (or anions) is smaller. These results are consistent with the consideration that strong Coulomb interactions between the cations and the anions enhance the possibility of approaching or attracting each other. Also, while the contribution of the momentum correlation between distinct cations, $P_1^{CC}(t)$, is smaller than that between the cation and anion molecules, $P_1^{CA}(t)$, the peak height of the $P_1^{CA}(t)$ in the polarizable model is larger than that in the nonpolarizable model. These results indicate that the transference of the momentum between distinct cations could be intensified by both charge-dipole and dipole-dipole interactions coming from polarization effects. As we could observe in the cross-

http://dx.doi.org/10.5772/51652

correlation functions (see Figures 4 and 5), the maxima of the momentum correlation functions between distinct cations emerge at earlier time region in comparison with those of the momentum correlations between cation and anion species.

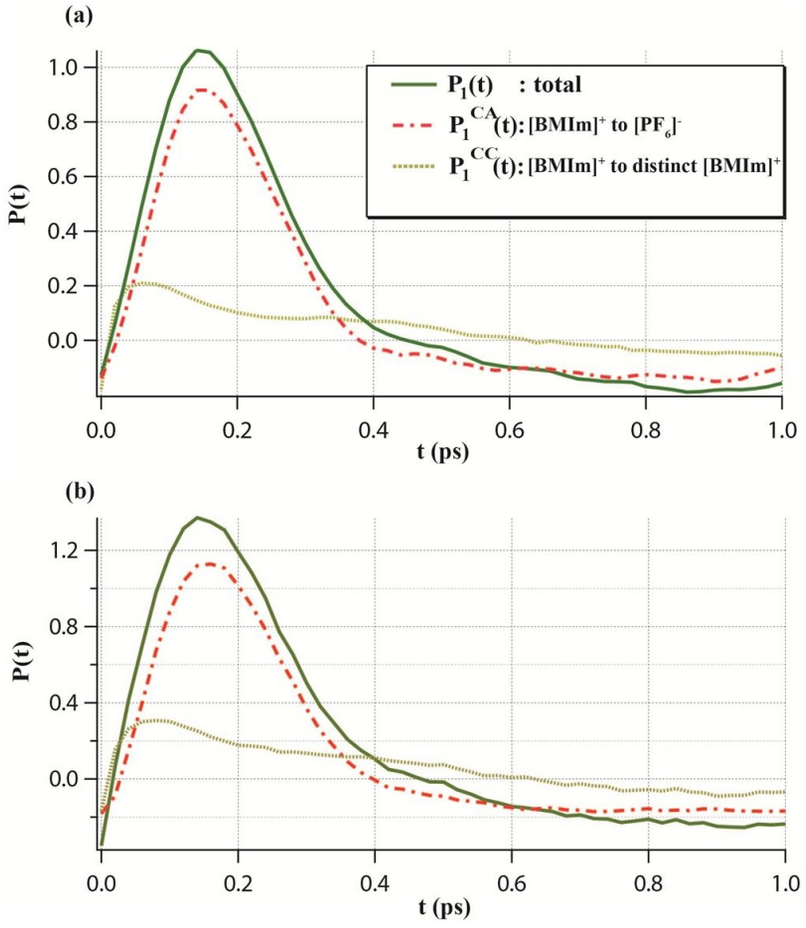

Figure 8. The calculated momentum correlation functions for the $[BMIm]^+$ at the center in the first coordination shell with the VACF: (a) in the nonpolarizable model and (b) in the polarizable model.

Based on these results, obviously, it is indicated that the variation of cage effects promotes the transfer of the initial momentum of the central cation to distinct cations rather than anions. Then, the cage effects is considered to be weakened by polarization effects, though the degree of this effect is likely to be relatively small as deduced from the figures.

On the other hand, the momentum correlations for the center anion in Figure 9 show distinct features from those for the center cation. The momentum correlation function between distinct anions, $P_1^{AA}(t)$, indicates much smaller contributions to the total momentum correlations, $P_1(t)$, in both the nonpolarizable and polarizable models, compared with the $P_1^{AC}(t)$. Therefore, these indicate that the initial momentum of the center anion is mainly transferred to neighboring cations, and the transference between distinct anions is not enhanced. These are consistent with the consideration that the cation-anion

interactions promote the propagation of the momentum one after another, as mentioned in the cation case. In addition, Figure 9 shows more interesting features. Compared with the results for the central cation in Figure 8, while the $P_1^{AA}(t)$ does not contribute negligibly to the total momentum correlation in the nonpolarizable model, it indicates characteristic oscillating behavior in the short time region up to 0.4 ps in the polarizable model, and the latter has a relatively larger contribution to the $P_1(t)$ up to 0.1 ps than in the nonpolarizable model. This clearly indicates the decrease of cage effects through polarization effects and implies that the interionic interactions between distinct anions could become effective by the charge-charge and dipole-dipole interactions [28].

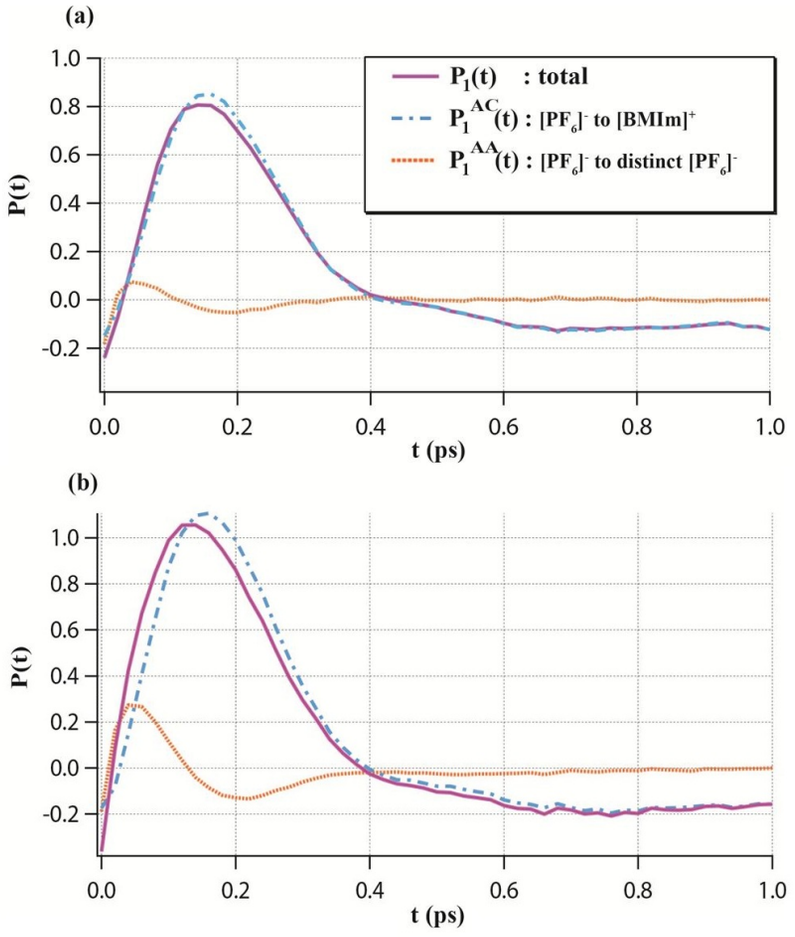

Figure 9. The calculated momentum correlation functions for the $[PF_6]^-$ at the center in the first coordination shell with the VACF: (a) in the nonpolarizable model and (b) in the polarizable model.

5. Relaxation Processes and Dynamical Properties

Firstly, the relaxation feature of IL system is examined with the computed polarizability TCF and its time derivative, and then, we discuss dynamical behavior of cations and anions

http://dx.doi.org/10.5772/51652

in ILs, and consider what kinds of properties with simulation data we have to check and care in the study of dynamical properties of ILs.

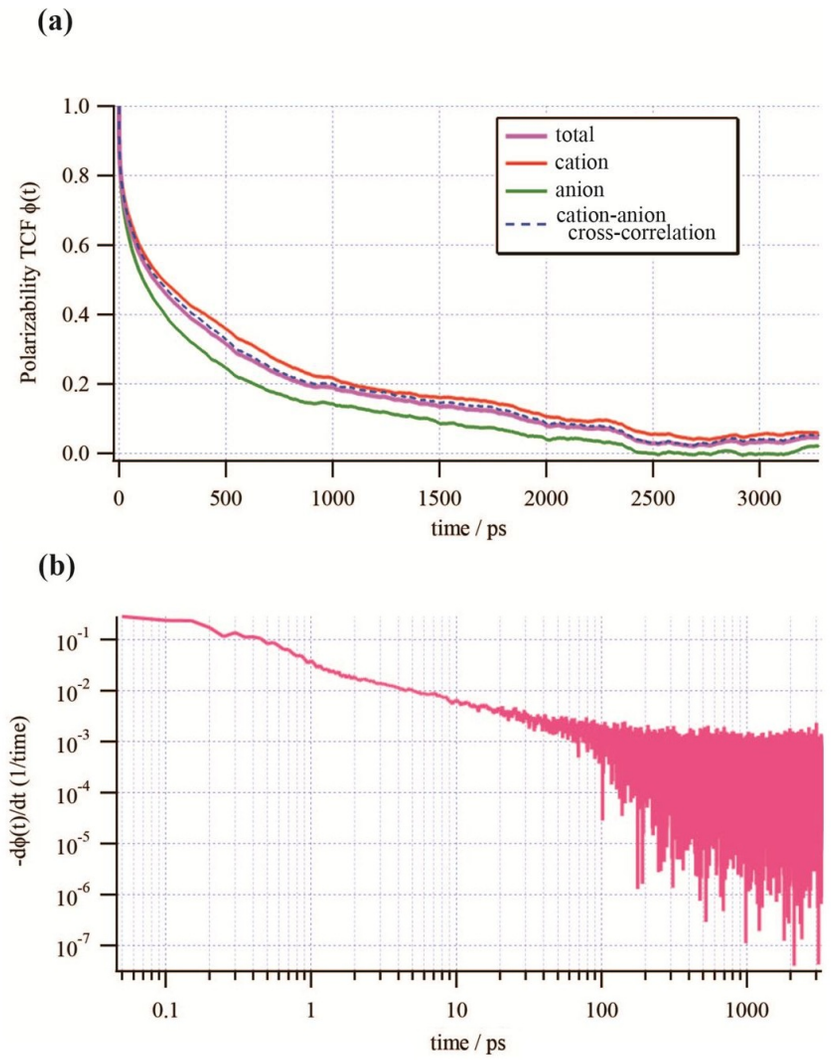

Figure 10. The computed polarizability TCF for each component (a) and the time derivative of the total polarizability TCF (b) for [BMIm][NTf_2] up to about 3 ns.

Figure 10 shows the computed polarizability TCF for each component and the time derivative of the total polarizability TCF for [BMIm][NTf_2]. As seen in Figure 10(a), the relaxation of the polarizability TCFs seems to be slower than in usual liquids. In particular, the relaxation of the anion shows faster decay than that of the cation. Also, for each component, it takes about 2~3 ns to approach toward zero. Thus, this indicates that it is required for us to perform a production MD simulation run for, at least, a few ns to study the relaxation behavior of the polarizability TCF. Also, as seen in Figure 10(a), the cation-anion cross-correlation indicates similar variation to the total polarizability TCF. Therefore, the relaxation behavior of the system strongly correlates with the cation-anion cross-correlation, and it is emphasized that tracking cross-correlation terms is very important. On the other hand, cor-

responding to this result, the time derivative of the polarizability TCF shows long-decay feature extending up to the nanosecond times, as seen in Figure 10(b). Considering that the time derivative of the polarizability TCF is directly related to optical Kerr effect (OKE) response,[14] these results are indicative of how long a MD simulation has to be carried out to examine the relaxation of the total system polarizability and the OKE response.

The relaxation process of ILs implies long-time dynamics of ILs. In particular, it has been known that diffusive motion of each ion in ILs at room temperature is usually much slower than in usual liquids.[1, 16] Therefore, a MD simulation would need to be run for a few ns or more. Then, we are able to use a procedure to check whether a system is in the diffusive regime. The procedure is to compute β(t) = dlog(MSD)/dlog(t),[16] where MSD means the mean-squared displacement (MSD) of the center of mass of ions, $\left\langle \sum_{i=1}^{N} [\boldsymbol{r}_i(t) - \boldsymbol{r}(0)]^2 \right\rangle$. In the case that β(t) = 1, the system is in the diffusive regime, while when b(t) < 1, the system is in the sub-diffusive regime. In Figure 11, computed β(t)s for [BMIm][NTf_2] are shown. These results indicate that both the cation and the anion reach the β(t) region between 0.8 and 1 (the shadowed area in Figure 11) after about 16 ns. This β(t) region is considered to be almost in the diffusive regime. Therefore, Figure 11 obviously indicates that, for confirming reliable self-diffusivities carefully, we need to perform a longer MD simulation than about 15 ~ 20 ns.

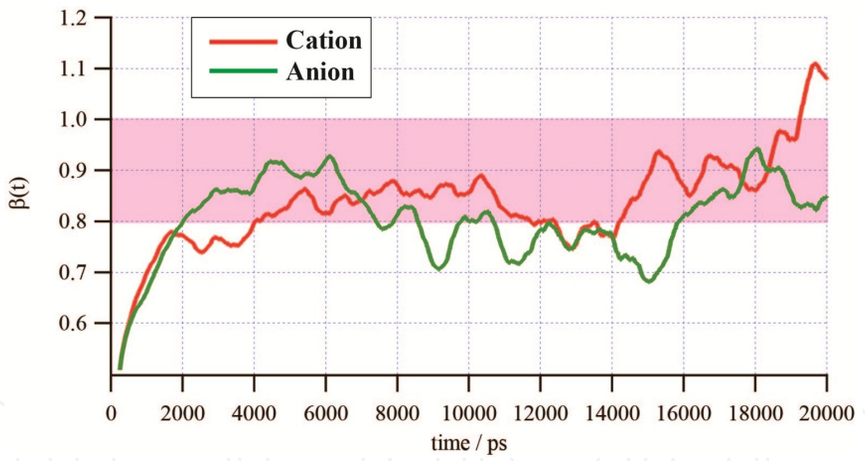

Figure 11. β(t) (see text) for $[BMIm]^+$ and $[NTf_2]^-$. Also, see text for the shadowed area.

Figure 12 displays the results calculated for the MSD and, in comparison, the non-Gaussian parameter, $\alpha(t)$, [50, 51]

$$\alpha(t) = 3\left\langle r^4(t)\right\rangle \Big/ 5\left\langle r^2(t)\right\rangle^2 - 1 \tag{32}$$

where $r(t)$ is the displacement of an ion at time t with respect to its position at t = 0. In Figure 12, the MSDs of $[PMIm]^+$ and $[NTf_2]^-$ indicate three typical dynamic ranges (regions), respec-

http://dx.doi.org/10.5772/51652

tively. Also, the behavior of the short- and long-time regimes of MSD for both the cation and the anion is similar to each other.

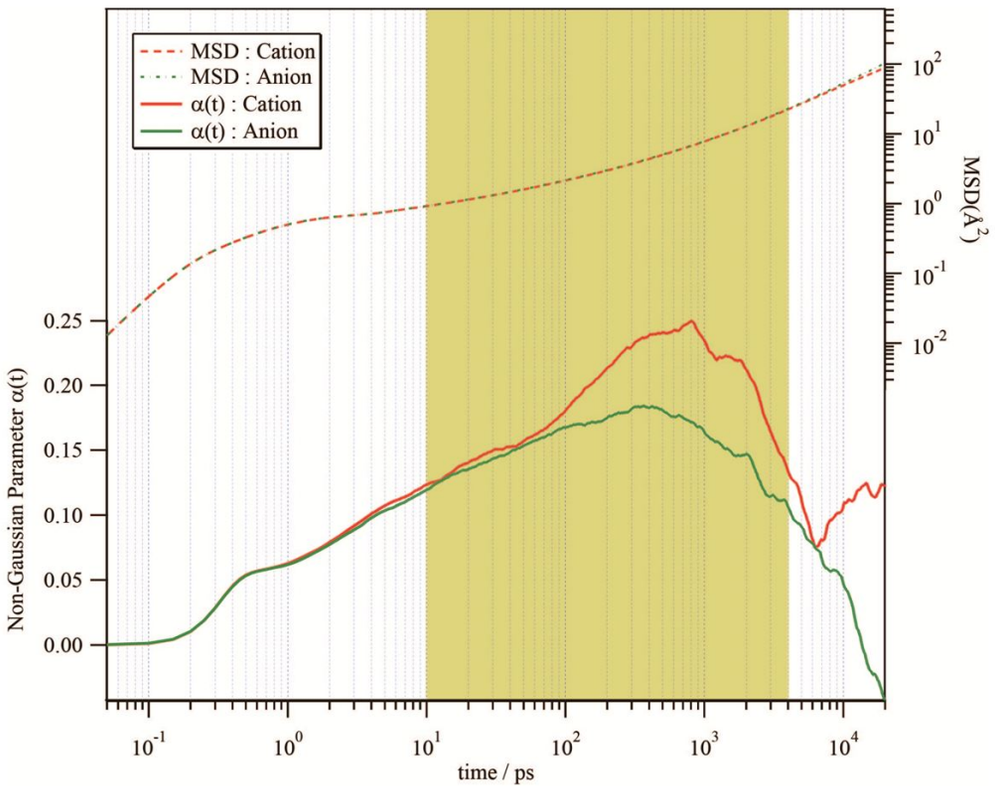

Figure 12. MSDs and non-Gaussian parameters for $[BMIm]^+$ and $[NTf_2]^-$. See text for the shadowed area.

For $[BMIm]^+$, first region is a microscopic regime until about 10 ps. Second is a crossover regime (the shadowed area in the Figure 12) until about 3-5 ns, and third regime is a sub-linear time dependence (sub-diffusive region) toward 20 ns. Also, $\alpha(t)$ has a double peak structure. One is at about 0.5 ps and the other at about 800 ps. In addition, a small shoulder structure emerges at between two peaks. As clearly seen in Figure 12, the short-time maximum peak corresponds to the microscopic region of the MSD, while the long-time maximum is located at around the center of the crossover regime of the MSD. On the other hand, for the anion, $[NTf_2]^-$, $\alpha(t)$ has a double peak structure similar to that of the cation. In particular, the long-time maximum peak is slightly shifted to about 300 ps, while the short-time maximum is locacted at the almost same time region as the cation. The time regime where the long-time maximum appear, is in good accord with those of $[BMIm]^+$, as shown in Figure 12. Therefore, considering that the magnitude of the deviation from the Gaussian behavior is remarkably larger for $[BMIm]^+$ than for $[NTf_2]^-$ as shown in Figure 12, it is expected that the relaxation behavior of the cation in perturbed $[BMIm][NTf_2]$ IL might be largely different from that of the anion. This consideration implies the possibility for us to find a distinct relaxation process in the OKE response (compare Figure 10 with Figure 12). Also, it should be noticed that the diffusive regime (linear

time-dependence region) after about 10 ns in Figure 12 coincides with the diffusive region in Figure 11 (after about 16 ns) for both the cation and the anion.

In particular, the shadowed area in Figure 12 covers the time range of the full width at half maximum (FWHM) of the second peak of $\alpha(t)$. As pointed out previously,[52] this FWHM range is likely to include a slow decay region usually known as the α relaxation which is characteristic of glass-forming supercooled liquids in general. Also, recently, it has been reported that similar behavior could appear for ILs at room temperature.[51, 53, 54] Therefore, we had better study the α relaxation in ILs with the observations of the non-Gaussian parameter in addition to information on spatial relaxation such as intermediate scattering function. Also, it is suggested that, when we investigate dynamical properties of ILs, the crossover, the sub-diffusive, and the diffusive regimes have to be carefully examined, as one of criterions for reliable research. Thus, only with a long-time MD simulation, it is considered that we are able to investigate dynamical properties of ILs to which experimental procedures are not accessible.

6. Conclusion

In this chapter, we introduced cross-correlation function analyses with a polarizable model, polarizability TCFs for investigating the relaxation behavior of ILs, and some of procedures for studying dynamical properties. We showed the importance of considering cross-correlation functions and related properties, showing some of examples. Firstly, we employed the polarizable model based on point dipole treatment to the investigation of the polarization effect on the target IL, [BMIm][PF_6]. With the MD simulation data for both the nonpolarizable and polarizable models, velocity cross-correlation analyses were shown, and we presented the momentum correlation functions between the cation and anion species in the IL. Next, we computed polarizability TCFs of [BMIm][NTf_2] and discussed their relaxation behavior. In addition, we investigated dynamical properties of ILs such MSDs and non-Gaussian parameters and considered what kinds of properties with simulation data we have to check and care in the study of dynamical properties of ILs. This chapter is summarized as follows:

1. In the study and discussion of velocity cross-correlation functions, it was shown that polarization effects could enhance the cross-correlations between $[BMIm]^+$ and $[PF_6]^-$ in the polarizable model in comparison with that in the nonpolarizable model. These features are ascribed to interionic interactions through attractive forces coming from the charge-dipole and dipole-dipole interactions caused by polarization effects in addition to charge-charge Coulomb interactions. Based on the results of computed cross-correlation between distinct cations (or anions), it was shown that, at early time region, the modulation of cage effects through polarization effects could improve the probability of approach between like ions. Also, by decomposing the cross-correlation function into the longitudinal and nonlongitudinal components, it was indicated that, at the short time region, the velocity cross-correlation is predominantly controlled by the longitudinal contribution. In addition, it was indicated that, compared with the

longitudinal correlation in the nonpolarizable model, the longitudinal component is further modified in the polarizable model.

2. On the momentum correlation functions between $[BMIm]^+$ and $[PF_6]^-$, it was exhibited that the correlation between $[BMIm]^+$ and $[PF_6]^-$ plays a important role. Also, it was shown that the contribution of the cross-correlation between distinct anions could be enhanced in the polarizable model. This result indicates that cage effects could be diminished with polarization effects, implying that the interionic interactions between distinct anions could be intensified by the charge-charge and dipole-dipole interactions related to polarization effects. Therefore, as has been pointed out in the literature [23, 24, 29], it is considered that the cage effect in ILs could be reduced by many-body polarization effects.

3. Both the computed polarizability TCF for each component and the time derivative of the total polarizability TCF for $[BMIm][NTf_2]$ showed long-time decay behavior. It was indicated that those took about 2~3 ns to approach toward zero. Therefore, this indicates that it is required for us to perform a production MD simulation run. Also, the relaxation behavior of ILs was investigated with the calculation of $\beta(t) = d\log(MSD)/d\log(t)$ as an indicator of the diffusive region. Our results suggested that long-time dynamics of ILs has to be studied with a longer MD simulation than about 15 ~ 20 ns for confirming reliable self-diffusivities in ILs, carefully. Furthermore, we examined MSDs and non-Gaussian parameters for $[BMIm][NTf_2]$. From our studies, it was exhibited that the magnitude of the deviation from the Gaussian behavior is remarkably larger for $[BMIm]^+$ than for $[NTf_2]^-$, and that, comparing with corresponding MSDs, it is possible to study diffusive motion of the cation and the anion. In addition, it was suggested that these studies imply the possibility for us to find a distinct relaxation process in the OKE response. Therefore, it is suggested that we had better study the α relaxation in ILs with the observations of the non-Gaussian parameter in addition to information on spatial relaxation such as intermediate scattering function. Lastly, it is concluded, only with a long-time MD simulation (> 15 ~ 20 ns), that we are able to investigate the dynamical properties of ILs to which experimental procedures are not accessible.

Acknowledgements

This work was supported in part by the Ministry of Education, Culture, Sports, Science and Technology (MEXT) of Japan (Grant-in Aid Scientific Research (C): 23550029).

Author details

Tateki Ishida*

Address all correspondence to: ishida@ims.ac.jp

Department of Theoretical and Computational Molecular Science, Institute for Molecular Science, Japan

References

[1] Wasserscheid, P., & Welton, T. (2008). *Ionic Liquids in Synthesis*, Weinheim, Wiley-VCH.

[2] Wasserscheid, P., & Keim, W. (2000). Ionic liquids- New "solutions" for transition metal catalysis. *Angew. Chem., Int. Ed.*, 39, 3773-3789.

[3] Castner, E. W. Jr, Wishart, J. F., & Shirota, H. (2007). Intermolecular Dynamics, Interactions, and Solvation in Ionic Liquids. *Acc. Chem. Res.*, 40, 1217-1227.

[4] Weingaertner, H. (2007). Understanding ionic liquids at the molecular level: facts, problems, and controversies. *Angew. Chem., Int. Ed.*, 47, 654-670.

[5] Ohno, H. (2005). *Electrochemical Aspects of Ionic Liquids*, Hoboken, Wiley-Interscience.

[6] Rogers, R. D., & Voth, G. A. (2007). Special Issue on Ionic Liquids. *Special Issue on Ionic Liquids. Acc. Chem. Res.*, 40(11).

[7] Wishart, J. F., & Castner, E. W. Jr. (2007). Special Issue on Physical Chemistry of Ionic Liquids.Special Issue on Physical Chemistry of Ionic Liquids. *Special Issue on Physical Chemistry of Ionic Liquids. J. Phys. Chem. B*, 111(18).

[8] Ohno, H., & Fukumoto, K. (2008). Progress in ionic liquids for electrochemical reaction matrices. *Electrochemistry*, 76, 16-23.

[9] Shirota, H., Wishart, J. F., Castner, E. W., & Jr , . (2007). Intermolecular Interactions and Dynamics of Room Temperature Ionic Liquids That Have Silyl- and Siloxy-Substituted Imidazolium Cations. *J. Phys. Chem. B*, 111, 4819-4829.

[10] Xiao, D., Rajian, J. R., Hines, J., , L. G., Li, S., Bartsch, R. A., & Quitevis, E. L. (2008). Nanostructural Organization and anion effects in the optical Kerr effect spectra of binary ionic liquids mixtures. *J. Phys. Chem. B*, 112, 13316-13325.

[11] Koeberga, M., Wu, C.-C., Kimc, D., & Bonn, M. (2007). THz dielectric relaxation of ionic liquid:water mixtures. *Chem. Phys. Lett.*, 439, 60-64.

[12] Yamamoto, K., Tani, M., & Hangyo, M. (2007). Terahertz Time-Domain Spectroscopy of Imidazolium Ionic Liquids. *J. Phys. Chem. B*, 111, 4854-4859.

[13] Shirota, H., Nishikawa, K., & Ishida, T. (2009). Atom substitution effects of $[XF6]^-$ in ionic liquids. 1. Experimental study. *J. Phys. Chem. B*, 113, 9831-9839.

[14] Ishida, T., Nishikawa, K., & Shirota, H. (2009). Atom substitution effects of $[XF6]^-$ in ionic liquids. 2. Theoretical study. *J. Phys. Chem. B*, 113, 9840-9851.

[15] Refer to the sec.4 in ref.1 and references therein.

[16] Maginn, E. J. (2007). Atomistic Simulation of the Thermodynamic and Transport Properties of Ionic Liquids. *Acc. Chem. Res*., 40, 1200-1207.

[17] Lopes, J. N. A. C., & Padua, A. A. H. (2006). Nanostructural Organization in Ionic Liquids. *J. Phys. Chem. B*, 110, 3330-3335.

[18] Bhargava, B. L., & Balasubramanian, S. (2007). Refined potential model for atomistic simulations of ionic liquid [bmim][PF_6]. *J. Chem. Phys*., 127(114510), 1-6.

[19] Znamenskiy, V., & Kobrak, M. N. (2004). Molecular Dynamics Study of Polarity in Room-Temperature Ionic Liquids. *J. Phys. Chem. B*, 108, 1072-1079.

[20] Shim, Y., Duan, J., Choi, M. Y., & Kim, H. J. (2003). Solvation in molecular ionic liquids. *J. Chem. Phys*., 119, 6411-6414.

[21] Kobrak, M. N. (2006). Characterization of the solvation dynamics of an ionic liquid via molecular dynamics simulation. *J. Chem. Phys*., 125(064502), 1-11.

[22] Hu, Z. H., & Margulis, C. J. (2006). Heterogeneity in a room-temperature ionic liquid: Persistent local environments and the red-edge effect. *Proc. Natl. Acad. Sci*., U.S.A., 103, 831-836.

[23] Yan, T., Burnham, C. J., Del Popolo, M. G., & Voth, G. A. (2004). Molecular Dynamics Simulation of Ionic Liquids: The Effect of Electronic Polarizability. *J. Phys. Chem. B*, 108, 11877-11881.

[24] Jiang, W., Yan, T., Wang, Y., & Voth, G. A. (2008). Molecular Dynamics Simulation of the Energetic Room-Temperature Ionic Liquid, 1-Hydroxyethyl-4-amino-1,2,4-triazolium Nitrate (HEATN). *J. Phys. Chem. B*, 112, 3121-3131.

[25] Urahata, S. M., & Ribeiro, M. C. C. (2005). Single particle dynamics in ionic liquids of 1-alkyl-3-methylimidazolium cations. *J. Chem. Phys*., 122(024511), 1-9.

[26] Urahata, S. M., & Ribeiro, M. C. C. (2006). Collective excitations in an ionic liquid. *J. Chem. Phys*., 124(074513), 1-8.

[27] Hu, Z., Huang, X., Annapureddy, H. V. R., & Margulis, C. J. (2008). Molecular Dynamics Study of the Temperature-Dependent Optical Kerr Effect Spectra and Intermolecular Dynamics of Room Temperature Ionic Liquid 1-Methoxyethylpyridinium Dicyanoamide. *J. Phys. Chem. B*, 112, 7837-7849.

[28] Ishida, T. (2011). Molecular dynamics study of the dynamical behavior in ionic liquids through interionic interactions. *J. Non-Cryst. Solids*, 357, 454-462.

[29] Leach, A. R. (2001). *Molecular Modeling, Principles and Applications*, Harlow, Pearson Education.

[30] Verdaguer, A., Padró, J. A., & Trullàs, J. (1998). Molecular dynamics study of the velocity cross-correlations in liquids. *J. Chem. Phys*., 109, 228-234.

[31] Verdaguer, A., & Padró, J. A. (2001). Computer simulation study of the velocity cross correlations between neighboring atoms in simple liquid binary mixtures. *J. Chem. Phys.*, 114, 2738-2744.

[32] Frenkel, D., & Smit, B. (2002). *Understanding Molecular Simulation, From Algorithms to Applications*, London, Academic Press.

[33] Bernardo, D. N., Ding, Y., Krogh-Jespersen, K., & Levy, R. M. (1994). An Anisotropic Polarizable Water Model: Incorporation of All-Atom Polarizabilities into Molecular Mechanics Force Fields. *J. Phys. Chem.*, 98, 4180-4187.

[34] Předota, M., Cummings, P. T., & Chialvo, A. A. (2002). Pair approximation for polarization interaction and adiabatic nuclear and electronic sampling method for fluids with dipole polarizability. *Mol. Phys.*, 100, 2703-2717.

[35] Ahlström, P., Wallqvist, A., Engström, S., & Jönsson, B. (1989). A molecular dynamics study of polarizable water. *Mol. Phys.*, 68, 563-581.

[36] Frenkel, D., & Mc Tague, J. P. (1980). Molecular dynamics studies of orientational and collision-induced light scattering in molecular fluids. *J. Chem. Phys.*, 72, 2801-2818.

[37] Geiger, L. C., & Ladanyi, B. M. (1987). Higher order interaction-induced effects on Rayleigh light scattering by molecular liquids. *J. Chem. Phys.*, 87, 191-202.

[38] Lopes, J. N. C., Deschamps, J, & Padua, A. A. H. (2004). Modeling Ionic Liquids Using a Systematic All-Atom Force Field. *J. Phys. Chem. B*, 108, 2038-2047.

[39] Lopes, J. N. C., Deschamps, J., & Padua, A. A. H. (2004). Additions and Corrections: Modeling Ionic Liquids Using a Systematic All-Atom Force Field. *J. Phys. Chem. B*, 108, 11250.

[40] Köddermann, T, Paschek, D, & Ludwig, R. (2007). Molecular Dynamic Simulations of Ionic Liquids: A Reliable Description of Structure, Thermodynamics and Dynamics. *ChemPhysChem*, 8, 2464-2470.

[41] Smith, W., & Forster, T. R. (2001). *The DL_POLY_2 User Manual*, Daresbury, United Kingdom, Daresbury Laboratory.

[42] Allen, M. P., & Tildesley, D. J. (1987). *Computer Simulation of Liquids*, Clarendon, Oxford.

[43] Shirota, H, Mandai, T, Fukazawa, H, & Kato, T. (2011). Comparison between Dicationic and Monocationic Ionic Liquids: Liquid Density, Thermal Properties, Surface Tension, and Shear Viscosity. *J. Chem. Eng. Data*, 56, 2453-2459.

[44] Nymand, T. M., & Linse, P. (2000). Ewald summation and reaction field methods for potentials with atomic charges, dipoles, and polarizabilities. *J. Chem. Phys.*, 112, 6152-6160.

[45] Van Duijnen, P. T., & Swart, M. (1998). Molecular and Atomic Polarizabilities: Thole's Model Revisited. *J. Phys. Chem. A*, 102, 2399-2407.

[46] Lide, D. R. (2006). *CRC Handbook of Chemistry and Physics*, Boca Raton, CRC Press.

[47] Thole, B. T. (1981). Molecular Polarizabilities Calculated with a Modified Dipole Interaction. *Chem. Phys.*, 59, 341-350.

[48] Molecular polarizabilities of [BMIm]+ and $[NTf2]^-$ were calculated with the same method in [14]. For molecular polarizability tensor elements of [BMIm]+, the reported values were used [14]. With the same procedures as in [14], molecular polarizability tensor elements of $[NTf2]^-$ were calculated, and the values of 9.8855, 1.4440×10^{-3}, $13.577\text{-}5\text{x } 10^{-4}$,-1.0539, and 10.315 $Å^3$ were used for α_{XX}, α_{XY}, α_{YY}, α_{XZ}, α_{YZ}, and α_{ZZ}, respectively.

[49] Verdaguer, A., & Padró, J. A. (2000). Velocity cross-correlations and atomic momentum transfer in simple liquids with different potential cores. *Phys. Rev. E*, 62, 532-537.

[50] Rahman, A. (1964). Correlations in the Motion of Atoms in Liquid Argon. *Phys. Rev.*, 136, A405-A411.

[51] Del Pópolo, M. G., & Voth, G. A. (2004). On the Structure and Dynamics of Ionic Liquids. *J. Phys. Chem. B*, 108, 1744-1752.

[52] Colmenero, J., Alvarez, F., & Arbe, A. (2002). Self-motion and the α relaxation in a simulated glass-forming polymer: Crossover from Gaussian to non-Gaussian dynamic behavior. *Phys. Rev. E*, 65(041804), 1-12.

[53] Ngai, K. L. (2011). *Relaxation and Diffusion in Complex Systems*, New York, Springer.

[54] Bhargava, B. L., Klein, M. L., & Balasubramanian, S. (2008). Structural Correlations and Charge Ordering in a Room-Temperature Ionic Liquid. *ChemPhysChem*, 9, 67-70.

IntechOpen